 doi:10.20944/preprints202011.0258.v1

An Experimental Investigation of Air-Acetic Acid Solution Gas-Liquid Two Phase in a Bubble Column

Wenlong Zhang, Shanglei Ning，Haibo Jin *, Guangxiang He, Lei Ma, Xiaoyan Guo, and Rongyue Zhang

Beijing Key Laboratory of Fuels Cleaning and Advanced Catalytic Emission Reduction Technology, School of Chemical Engineering, Beijing Institute of Petrochemical Technology, Beijing 102617, China;

***Correspondence: jinhaibo@bipt.edu.cn; Tel.: +86-010-81292208**

Abstract: The hydrodynamic behavior of the air-acetic acid system in a bubble column is studied using a differential pressure transmitter, double probe optical fiber probe, and the electrical resistance tomography (ERT) technique. The superficial gas velocity ranges from 0.016 to 0.094 m/s under ambient temperature and pressure. The influences of viscosity and surface tension on gas holdup, bubble rising velocity, and bubble chord distribution in the column are discussed with different mass fractions of an acetic acid solution. The results show that as the mass fraction of acetic acid increases, the surface tension of the liquid phase decreases, and the viscosity first increases and then decreases. This causes the gas holdup in the column to first increase and then decrease, and reaches the maximum value at an acetic acid mass fraction of 55% to 60%. The rising velocity of the bubbles in the column is high in the central region and has a low-value distribution near the wall. The bubble chord length distribution is concentrated, and the distribution of the bubble chord length in the column becomes narrow with any decrease in surface tension. Studying the hydrodynamic behavior of a bubble column with the air-acid system is of great significance considering the absence of data on air-organic acid systems.

Keywords: air-acetic acid system; gas holdup; differential pressure transmitter; ERT; optical fiber probe

 doi:10.20944/preprints202011.0258.v1

1. Introduction

Bubble column reactors have been widely used in petrochemical, chemical, biochemical, and pharmaceutical industries [1-3], with the advantages of a simple construction, no mechanically moving parts, good mass transfer properties, high thermal stability, low energy supply, and low operation costs [4-6]. The characteristics of the bubble are the most important parameters in the bubble column; they can be used to estimate the average residence time of bubbles and the contact area of the gas and liquid phases to determine the mass transfer intensity and the reaction rate of the column. The factors that affect the gas holdup in the bubble column reactor are temperature, pressure, liquid properties (density, viscosity, and surface tension), and the distributor and size of the bubble column. The influence of liquid viscosity and surface tension on gas holdup is highly complex, affecting any change in hydrodynamic behavior in the column. Therefore, it is necessary to fully understand the effects of changes in the physical properties of liquids in the column.

Liquid properties such as liquid viscosity and surface tension play important roles in hydrodynamics and bubble coalescence and breakup. The effects of liquid viscosity have been studied and it has been found that an increase in liquid viscosity significantly inhibits bubble breakup at higher liquid viscosities and enhances bubble coalescence at low levels of viscosity [7-9]. Xing et al. [10] studied the effect of the viscosity of a glycerin solution on hydrodynamic behavior through experimental research and numerical simulation and found that the effect of liquid viscosity on bubble coalescence is less significant than its effect on bubble breakup. Besagni et al. [11] studied air-glycol systems with viscosities between 0.9 mPa·s and 7.97 mPa·s and found that liquid viscosity has a dual effect. With increases in viscosity, the gas holdup first increases and then decreases, and there is a maximum. Ruzicka et al. [12] found that the gas holdup increased with an increase in viscosity at 0–3 mPa·s, but the gas holdup began to decrease at a range of 3–22 mPa·s. Olivieri et al. [13] used a sodium alginate aqueous solution at a viscosity range of 1–117 mPa·s to study the influence of liquid viscosity and their results show that the gas holdup is largest when μ_l = 4.25 mPa·s, and then, as the viscosity increased, the gas holdup began to decrease. The relevant properties of the surface tension also significantly affect bubble behavior. In the liquid phase, the total gas holdup increases with a decrease in surface tension. The reason for this is that in the liquid phase, the change in surface tension affects the coalescence and breakup behavior. With decreasing surface tension, the bubble breakup is enhanced and the bubble coalescence is inhibited, which in turn reduces bubble size and increases gas holdup.

The oxidation reaction process of p-xylene uses acetic acid as the solvent in the bubble column reactor. Changes in the physical properties of the acetic acid system have a significant influence on the gas holdup in the column; therefore, the study of hydrodynamic behavior in an air-acetic acid system has a certain significance in the design and enlargement of a bubble column. In addition, the p-xylene oxidation reactor is the key equipment that affects the production of terephthalic acid in industrial processes. There are few studies on oxidation bubble columns with an organic solution. Therefore,

Based on the background of p-xylene oxidation reactors in terephthalic acid production, this work aims to systematically study the effects of viscosity and surface tension on the holdup of gas. At a superficial gas velocity range of 0.016 to 0.094 m/s, the gas holdup, bubble rising velocity, and bubble chord length distribution in the column are measured using differential pressure transmitters, fiber optic probes, electrical resistance tomography (ERT), and other technologies. The drift flux method is used to further study the influence of a different mass fraction of acetic acid on the flow regime transition point. This paper focuses on the behavior of the bubble column at different acetic acid concentrations, and provides the basis for the selection and optimization of industrial operation parameters.

Preprints (www.preprints.org) | NOT PEER-REVIEWED | Posted: 8 November 2020 doi:10.20944/preprints202011.0258.v1

2. Experimental procedure

2.1 Experimental apparatus

The experimental equipment consists of a cylindrical bubble column with a diameter of D = 150 mm and a height of H = 2300 mm, and the initial static liquid level H_0 = 1150 mm, as shown in Figure 1. There are a total of ϕ 2 mm × 19 on the gas distributor, and the opening rate is approximately 0.338%. Two holes are opened at the column heights H_1 = 0.76 m and H_2 = 0.86 m to collect experimental data using differential pressure transmitters [14, 15], optical fiber probes [16], and ERT [17-19].

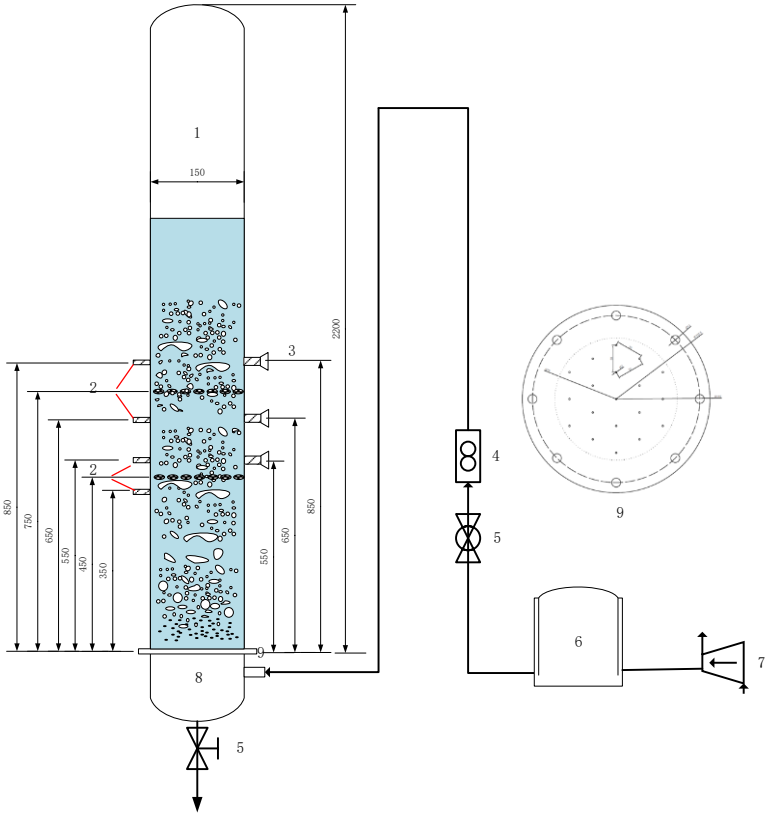

Figure 1 Experimental device diagram of a 150 mm bubble column.

1 Glass bubble column; 2 Differential pressure transmitter; 3 Optical fiber probe measurement position; 4 Rotameter; 5 Valve; 6 Gas storage tank; 7 Fan; 8 Gas chamber; 9 Porous plate gas distributor.

2.2 The properties of acetic acid

In the experiment, acetic acid solutions of different concentrations from industrial acetic acid (100% acetic acid) were prepared. The density, surface tension, and viscosity of the solution were measured, and the physical properties are shown in Table 1.

Table 1 Physical properties of acetic acid with different mass fractions.

Concentration (wt. %)	Density/ρ ($kg \cdot m^{-3}$)	Viscosity/μ (mPa·s)	Surface Tension/σ ($\times 10^{-3} N \cdot m^{-1}$)
0	998	1.00	72.0
1	1000	1.08	68.0

Preprints (www.preprints.org) | NOT PEER-REVIEWED | Posted: 8 November 2020 doi:10.20944/preprints202011.0258.v1

2	1001	1.09	64.5
3	1003	1.10	63.2
4	1004	1.12	62.3
5	1006	1.13	60.1
10	1013	1.22	54.5
15	1020	1.34	51.2
20	1026	1.45	47.7
25	1033	1.58	45.7
30	1038	1.70	43.6
35	1044	1.83	42.2
40	1049	1.96	40.7
45	1053	2.08	39.6
50	1058	2.21	38.4
55	1061	2.32	37.4
60	1064	2.43	36.3
65	1067	2.54	35.2
70	1069	2.66	34.2
75	1070	2.69	33.0
80	1070	2.75	31.9
85	1069	2.57	30.6
90	1066	2.43	29.4
95	1061	1.81	28.0
100	1050	1.22	26.6

In Table 1, the surface tension of the liquid gradually decreases with the increase in the acetic acid mass fraction. The viscosity of the liquid gradually increases with the increase in the acetic acid mass fraction. When the mass fraction reaches 80%, the viscosity is at its highest, before rapidly declining. Understanding the characteristics of acetic acid solutions with different mass fractions can help to accurately understand the reasons behind changes in hydrodynamic parameters in the bubble column.

2.2 Measurement method

2.2.1 Differential Pressure Transmitter

The average gas holdup between the two sections is obtained through a differential pressure transmitter. The measurement principle is shown in the following formula：

Preprints (www.preprints.org) | NOT PEER-REVIEWED | Posted: 8 November 2020 doi:10.20944/preprints202011.0258.v1

$$\varepsilon_g = \frac{\Delta P}{(\rho_l - \rho_g) g \Delta H} \approx \frac{\Delta P}{\rho_l g \Delta H} \tag{1}$$

where ΔP is the differential pressure between the two sections, ρ_l is the liquid density, ρ_g is the gas density, g is the acceleration of gravity, and ΔH is the vertical distance between the two measurement sections.

2.2.2 Fiber Optic Probe

The dual fiber probe is an invasive measurement device that can measure a series of data, including gas holdup, bubble chord length, and bubble rising velocity. The typical measurement signal is shown in Figure 2. During the measurement process, when the fiber tip position is in the gas phase, the light is reflected completely. When it is in the liquid phase, the emitted laser light is partially absorbed by the liquid phase, which causes the intensity of the received laser light to be different. A series of photoelectric conversions is carried out by the collection device, the measured signal is amplified, and, finally, A/D conversion is performed to complete the data collection and to obtain the time series of the optical fiber signal changes [20, 21].

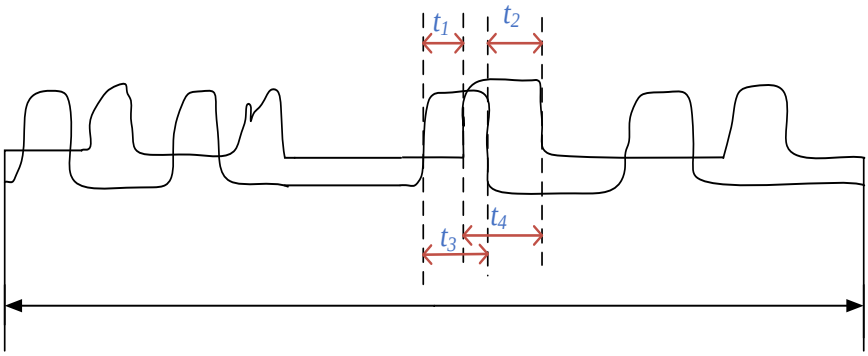

Figure 2 Typical signals during fiber probe measurement.

The average gas holdup in a column can be obtained by dividing the gas holdup measured at different radial positions by the cross-sectional area of the column. The specific expression is shown in Equation (2):

$$\varepsilon = \frac{2\pi \int_0^R \varepsilon r dr}{\pi R^2} \tag{2}$$

As shown in Figure 2, the measurement of bubble rising velocity is mainly based on the time difference between the two sensors' output signals. The specific expression is shown in Equation (3):

$$U_b = \frac{2L}{t_1 + t_2} \tag{3}$$

where L is the distance between the two probes, and t is the time it takes for the bubble to pass through the probe.

The bubble chord length is mainly determined based on the bubble rising velocity, and the bubble is recorded by the probe. The expression is as follows:

$$L_b = \frac{U_b(t_3 + t_4)}{2} \tag{4}$$

Preprints (www.preprints.org) | NOT PEER-REVIEWED | Posted: 8 November 2020 doi:10.20944/preprints202011.0258.v1

2.2.3 Electrical Resistance Tomography

The measurement principle of electrical resistance tomography (ERT) is to inject current between adjacent electrode pairs, stimulate the current, and measure the voltage generated on the remaining adjacent electrode pairs. After the voltage measurement value is obtained from the sensor, the image reconstruction algorithm can use to process the data.

ERT can convert conductivity data into gas holdup using Maxwell's equation. The specific conversion method is shown in Equation (5):

$$\varepsilon = \frac{2\lambda_1 + \lambda_2 - 2\lambda_{mc} - \frac{\lambda_{mc}\lambda_2}{\lambda_1}}{\lambda_{mc} - \frac{\lambda_2}{\lambda_1}\lambda_{mc} + 2(\lambda_1 - \lambda_2)} \tag{5}$$

where λ_1 is the conductivity of the continuous phase (mS/cm), λ_2 is the conductivity of the dispersed phase (mS/cm), and λ_{mc} is the conductivity value measured during the experiment.

In the gas-liquid two-phase experimental system, the dispersed phase is air, and the conductivity value is 0; that is, $\lambda_2 = 0$. Therefore, the equation of gas holdup is as shown in Equation (6):

$$\varepsilon = \frac{2\lambda_1 - 2\lambda_{mc}}{\lambda_{mc} + 2\lambda_1} \tag{6}$$

3. Results and Discussion

3.1 Gas Holdup

3.1.1 Average Gas Holdup

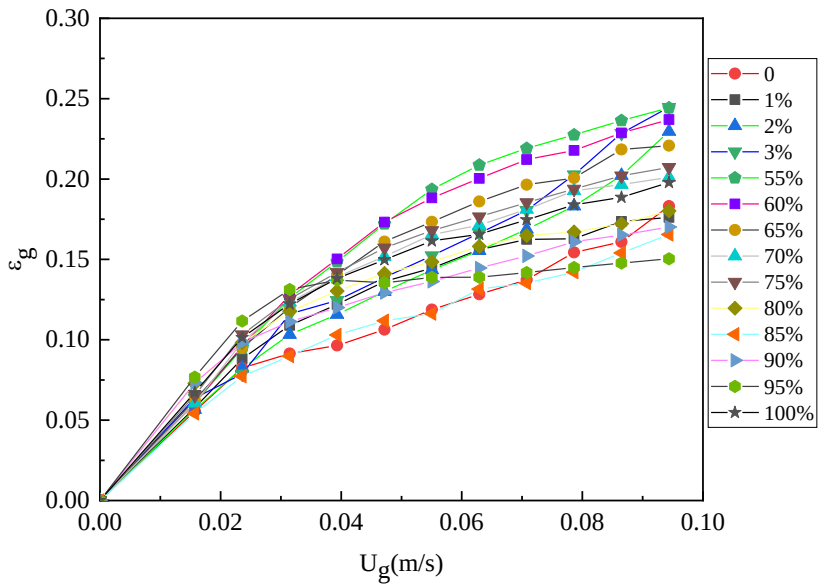

Figure 3 Effect of different concentrations of acetic acid on the gas holdup in the column.

The relationship between the average gas holdup measured by a differential pressure transmitter and the superficial gas velocity under different acetic acid concentrations is as shown in Figure 3. With

Preprints (www.preprints.org) | NOT PEER-REVIEWED | Posted: 8 November 2020 doi:10.20944/preprints202011.0258.v1

an increase in superficial gas velocity, the gas holdup in the column gradually increases. Furthermore, when the acetic acid concentration gradually changes from a low concentration to a high concentration, the gas holdup in the column gradually increases. When the concentration of acetic acid reaches 55% or 60%, the gas holdup in the column is at its highest level. However, when the concentration of acetic acid is further increased, the gas holdup begins to decline slowly, which shows the dual influence of the concentration on gas holdup. The main reason for this is that with the increasing concentration of the acetic acid solution, the physical properties of the acetic acid solution change. From Table 1, when the concentration of acetic acid changes from a low concentration to a high concentration, the density of the solution gradually increases and the viscosity gradually increases. However, when the concentration reaches 80%, the viscosity drops sharply and the surface tension gradually decreases. Among the general influence characteristics from these three physical properties, the density of the liquid increases, the gas holdup increases； the viscosity increases, the gas holdup first increases and then decreases; the surface tension decreases, the gas holdup increases. They have a comprehensive effect on the gas holdup.

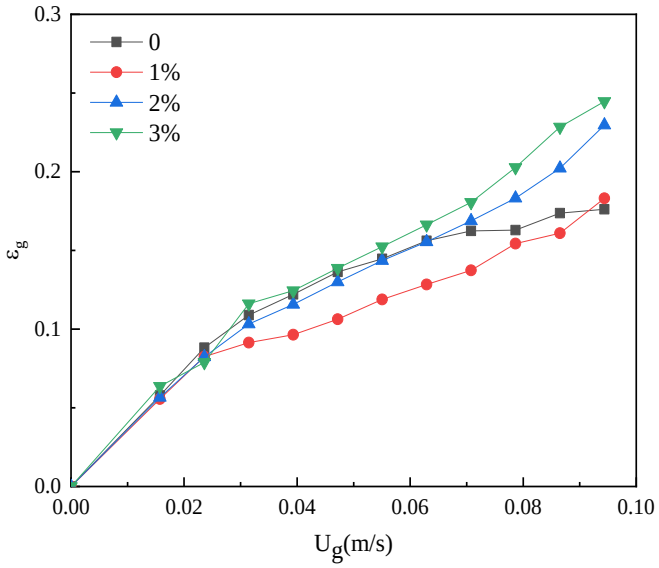

Figure 4 Effect of 0–3% concentrations of acetic acid on the gas holdup in the column.

Figure 4 shows the influence of 0, 1%, 2%, and 3% mass fractions of acetic acid on gas holdup. As the concentration of acetic acid increases, the gas holdup in the column gradually increases. The main reason for this is the decrease in the surface tension and the increase in the viscosity of the solution. The decrease in surface tension increases the instability of the bubbles in the column, which cause the large bubbles to break into small bubbles, and the gas holdup increases. Besagni et al. [14] suggested that in a low-viscosity solution, an increase in viscosity leads to an increase in drag force, which further reduces the rising velocity of bubbles and increases the gas holdup in the column. Therefore, the gas holdup gradually increases with the increase in solution concentration in the range of low acetic acid concentrations.

Preprints (www.preprints.org) | NOT PEER-REVIEWED | Posted: 8 November 2020 doi:10.20944/preprints202011.0258.v1

3.1.2 Images of cross-section gas holdup using ERT

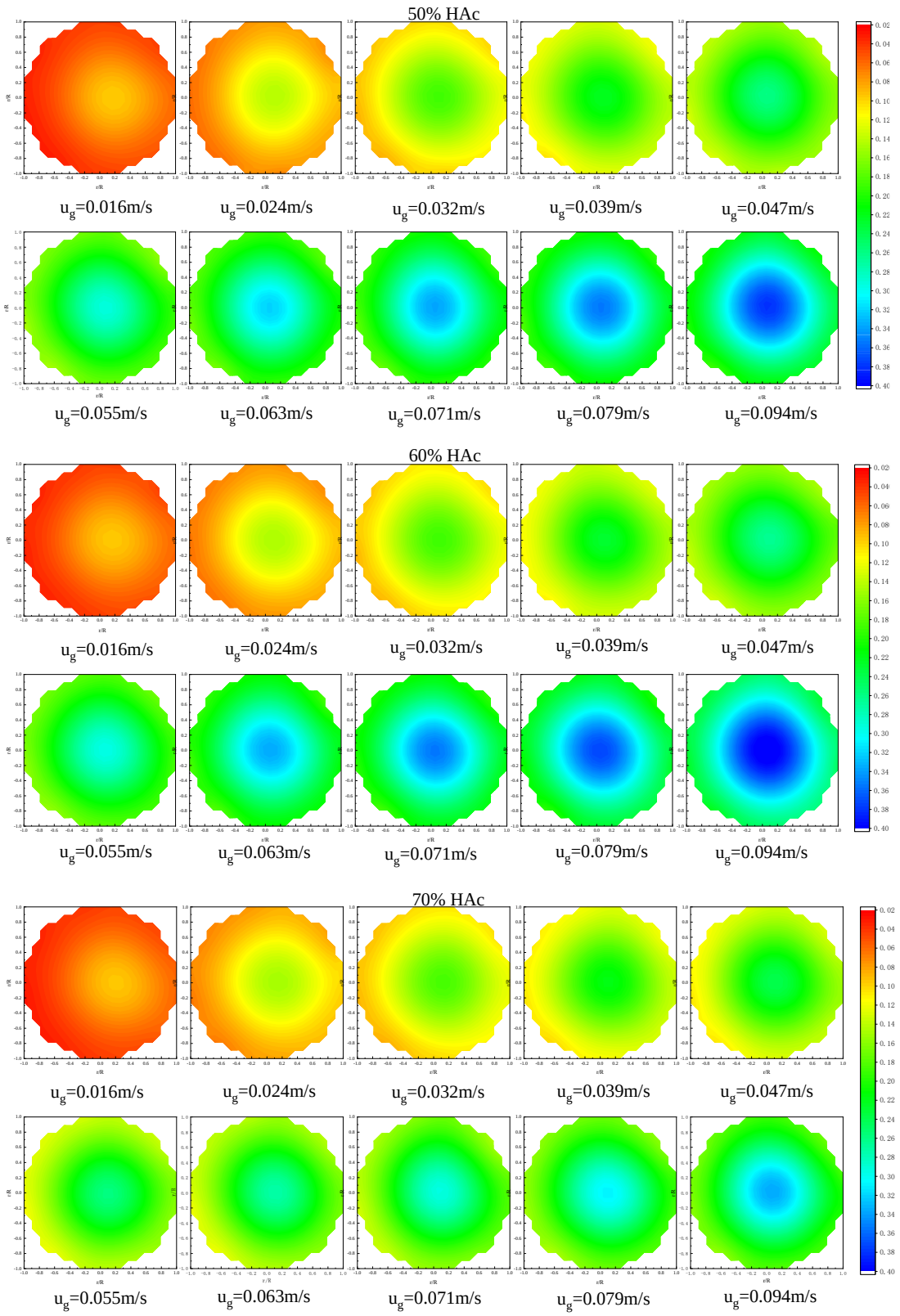

Preprints (www.preprints.org) | NOT PEER-REVIEWED | Posted: 8 November 2020 doi:10.20944/preprints202011.0258.v1

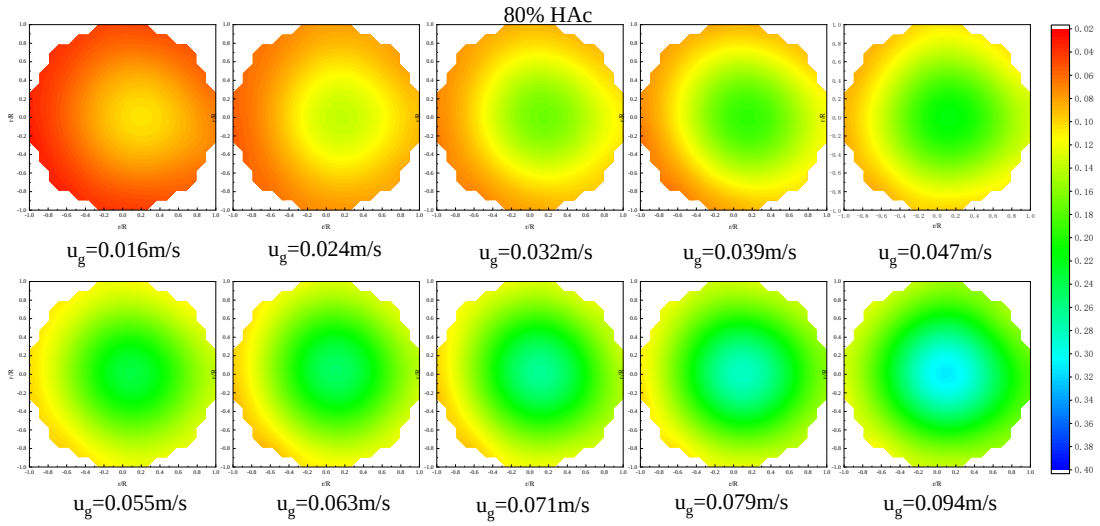

Figure 5 Gas holdup distribution diagram measured by ERT.

Figure 5 shows a gas holdup cross-section distribution diagram of 50%-80% concentrations of acetic acid using the ERT technique. To visualize the influence of different acetic acid concentrations and different superficial gas velocities on the gas holdup, a unified legend is used to illustrate changes in gas holdup. It can be seen that the gas holdup varies from 0.02 to 0.40, in which red represents a low gas holdup value and blue represents a high gas holdup value. It is observed that with the increase in the superficial gas velocity, the red area in the image gradually decreases, and the blue area gradually expands. This further indicates that with an increase in the superficial gas velocity, the gas holdup increases gradually at a certain concentration, and the gas holdup in the column increases gradually.

At the same time, by observing the color difference in the same superficial gas velocity at different concentrations, the influence of acetic acid at different concentrations on the gas holdup in the column can be obtained. It can be seen from Figure 5 that when the acetic acid concentration is 60%, the central gas holdup in the column is relatively large.

3.1.3 Radial gas holdup distribution

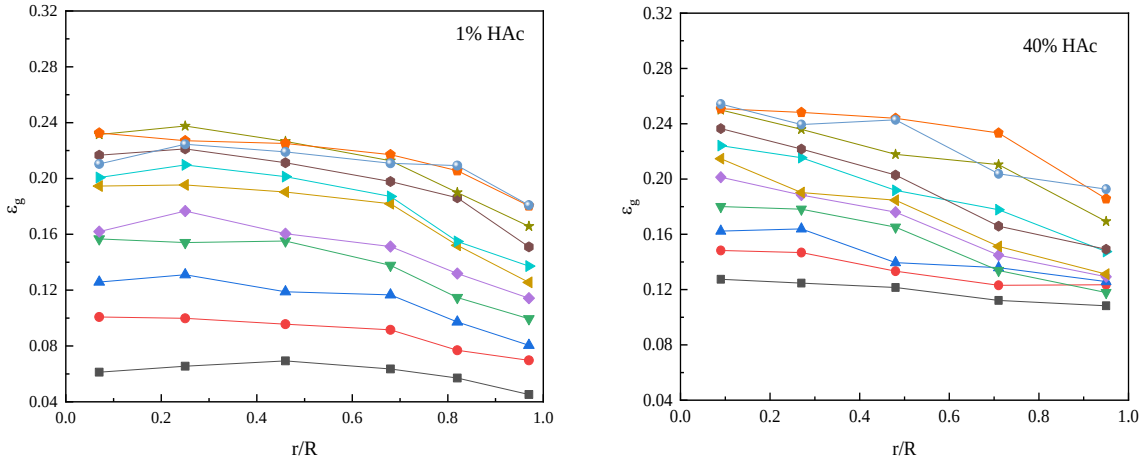

Preprints (www.preprints.org) | NOT PEER-REVIEWED | Posted: 8 November 2020 doi:10.20944/preprints202011.0258.v1

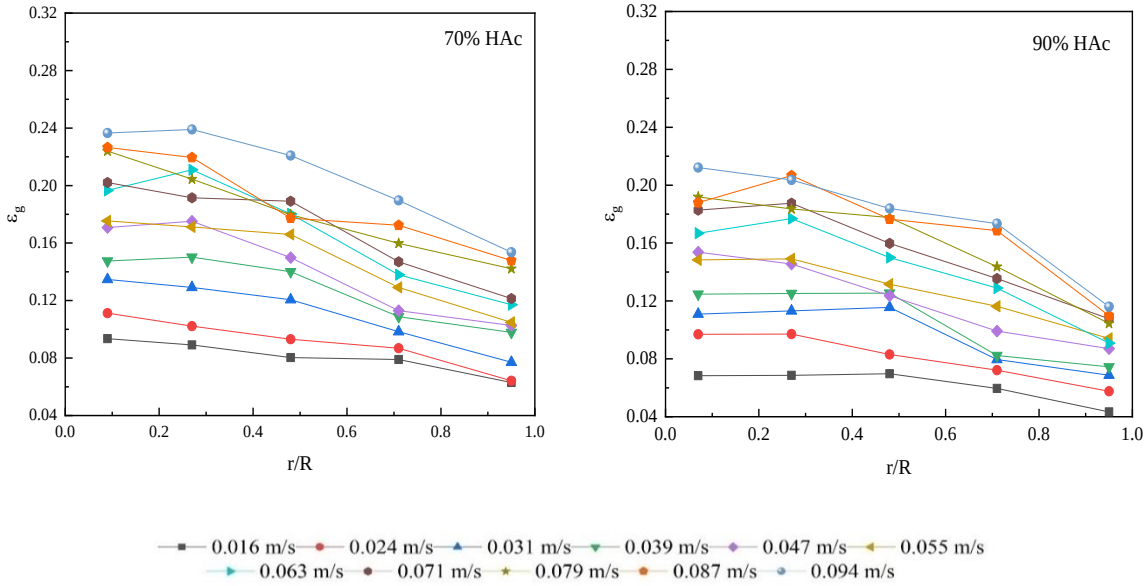

Figure 6 Effect of acetic acid concentration on radial gas holdup.

The radial gas holdup can reflect the uniformity of gas-liquid mixing in the bubble column, which is of great significance to understanding the reaction of mass transfer and heat transfer. Figure 6 shows variations of gas holdup at different radial positions with a superficial gas velocity on a 1%, 40%, 70%, and 90% air-acetic acid solution system. It is generally believed that the radial gas holdup of the gas-liquid bubble column is symmetrically distributed. Through comparison, it can be found that at a low superficial gas velocity, the radial gas holdup distribution is relatively uniform, the force between the bubbles in the column is small, and the column is in the homogeneous regime. With a gradual increase in the superficial gas velocity, the flow regime changes, and the bubbles in the column coalesce and breakup so that the gas holdup is at its highest in the center of the column and gradually decreases toward the wall. This distribution law is consistent with records in the literature [22]. In terms of the gas holdup at the same radial position, the gas holdup gradually increases with an increase in the superficial gas velocity. The influence of the change in viscosity caused by the change in acetic acid concentration on radial gas retention is also twofold. At concentrations of 1%, 40%, 70%, and 90%, as the concentration of acetic acid increases, the radial gas holdup gradually increases. When the acetic acid concentration is 40%, the measured radial gas holdup value is at its largest. As the acetic acid concentration further increases, the radial gas holdup gradually decreases, mainly due to the increase in viscosity, which causes bubbles to coalesce and form larger bubbles, thereby accelerating the bubble rising velocity.

Preprints (www.preprints.org) | NOT PEER-REVIEWED | Posted: 8 November 2020 doi:10.20944/preprints202011.0258.v1

3.2 Bubble rising velocity

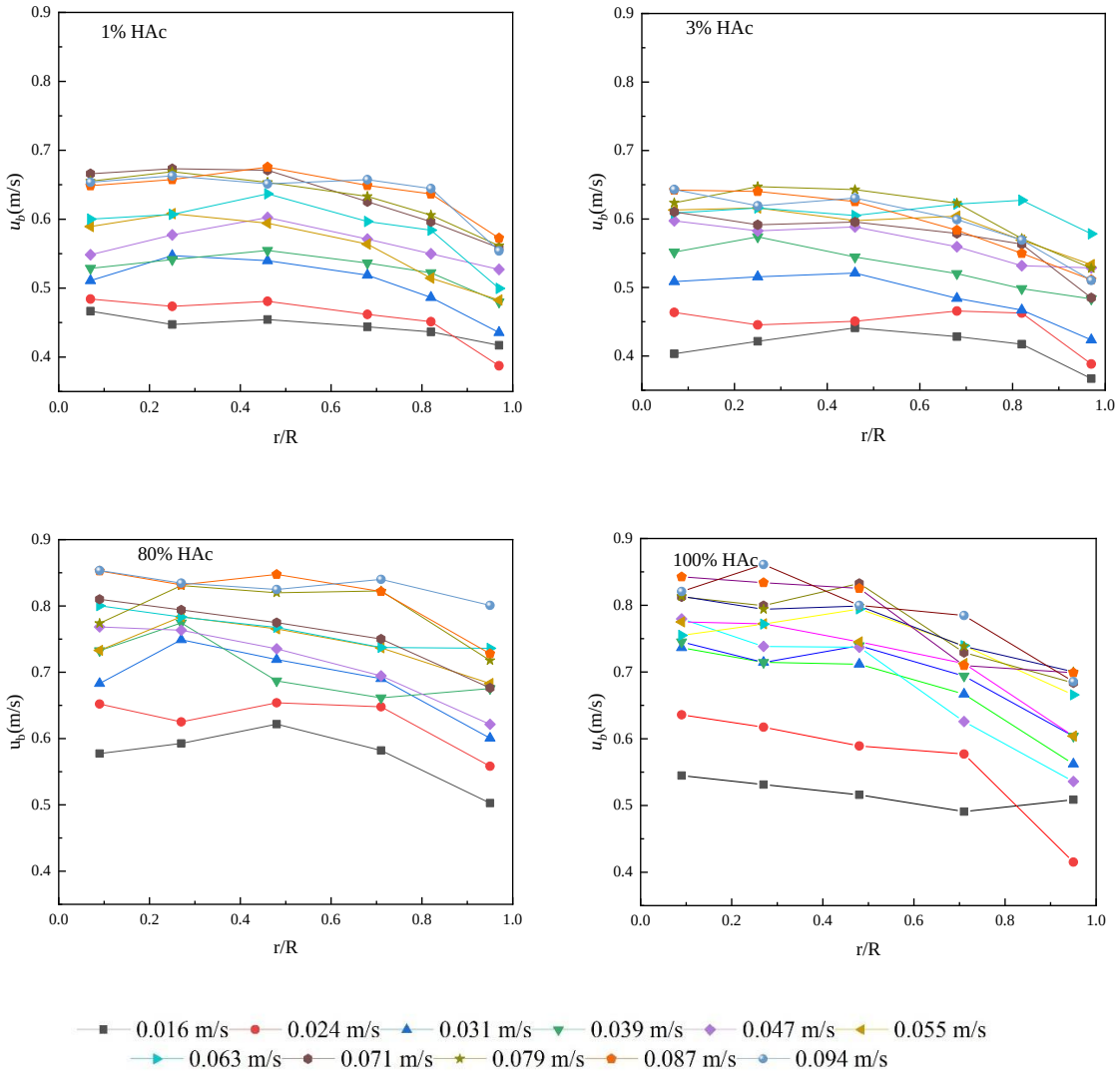

Figure 7 Effects of different concentrations of acetic acid on bubble rising velocity.

The bubble rising velocity measured at 1%, 3%, 50%, and 100% acetic acid concentrations is shown in Figure 7. It can be seen that the rising velocity of bubbles increases with an increase in superficial gas velocity at different acetic acid concentrations. The rising velocity is highest near the center of the column. In addition, the change in acetic acid concentration can cause a significant change in bubble rising velocity. It is generally believed that the higher the rising velocity of bubbles, the shorter the time the bubbles reside in the column and the lower the gas holdup in the column. It can also be seen from Figure 7 that when the concentration is 3%, the bubble rising velocity is relatively small, but the bubble rising velocity is large at a lower concentration of 1% and at other high-concentration solutions. This result further illustrates the relationship between gas holdup and bubble rising velocity.

3.3 The distribution of the bubble chord length

The size of the bubble and the gas holdup determine the area of the gas-liquid interface, which is essential for the correct design and optimization of the bubble column. In the experiment, the fiber probe is used to measure the bubble chord length at different radial positions under different acetic acid

Preprints (www.preprints.org) | NOT PEER-REVIEWED | Posted: 8 November 2020 doi:10.20944/preprints202011.0258.v1

concentrations, and the measured results are arranged into a relative frequency distribution diagram of the bubble chord length to further understand the variation of bubble chord lengths at different superficial gas velocities and different radial positions in the column.

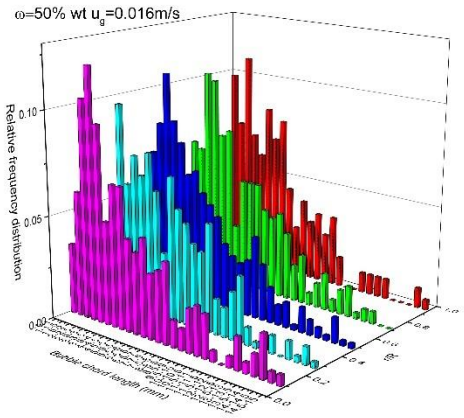

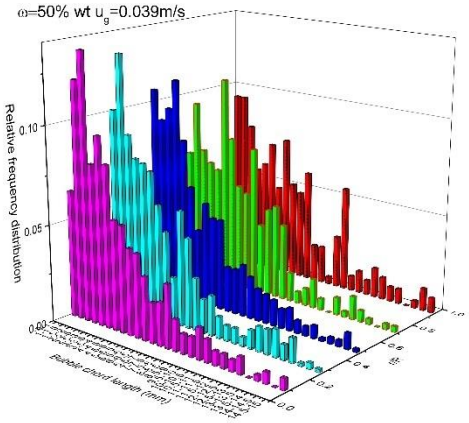

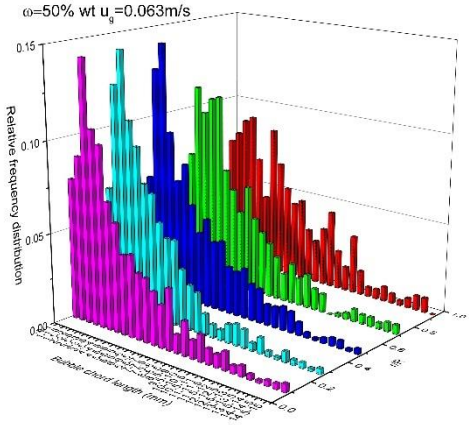

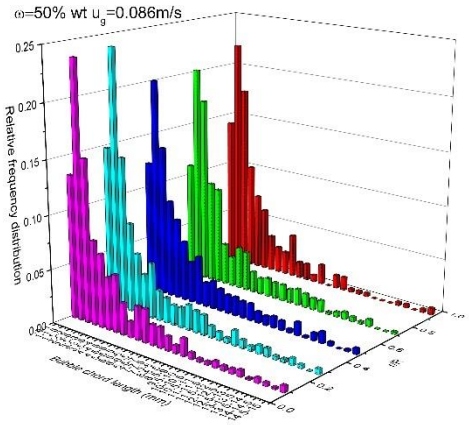

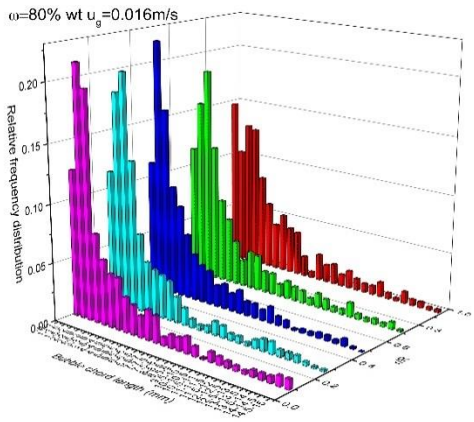

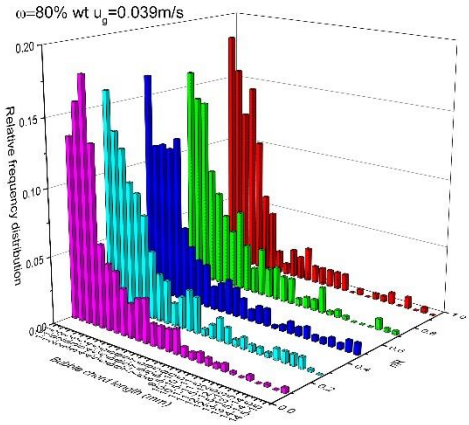

Preprints (www.preprints.org) | NOT PEER-REVIEWED | Posted: 8 November 2020 doi:10.20944/preprints202011.0258.v1

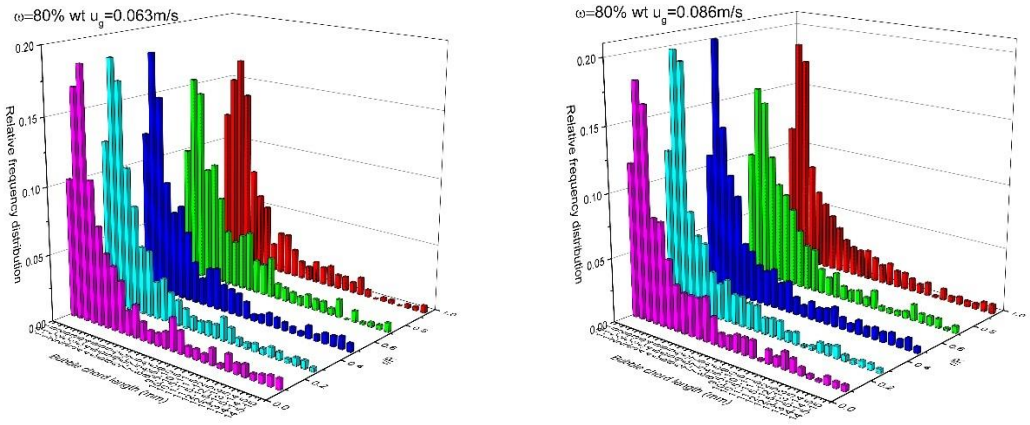

Figure 8 Relative frequency distribution diagrams of the bubble chord length in different acetic acid solutions.

Figure 8 shows the probability distribution of a bubble chord length at different radial positions of acetic acid solutions with mass fractions of 50% and 80% when the apparent gas velocities are 0.016 m/s, 0.039 m/s, 0.063 m/s, and 0.086 m/s, respectively. It can be seen that at a certain concentration of acetic acid, the probability distribution of bubble chord lengths is mostly concentrated in the same area, and gradually decreases with the increase in the radial position parameter r/R. Most of the bubbles in the bubble column are concentrated in the central regime; the closer to the wall they are, the fewer bubbles exist and the smaller the probability distribution of chord length. Most researchers [23-25] believe that lift force may be pushing "small" bubbles away from the center of the column. At the same concentration, as the superficial gas velocity increases, the probability distribution of the bubble chord length also gradually increases. It can also be observed in Figure 8 that different concentrations of acetic acid will also affect the probability distribution of the chord length in the column, which in turn causes the chord length size and main distribution area to change. The main reason for this phenomenon is the change in the liquid properties, which in turn affects the coalescence and breakup of bubbles, and finally leads to the change in bubble chord length.

3.4 The flow regime

The flow regime in the bubble column is generally divided into a homogeneous regime, transition regime, and heterogeneous regime. The transition of the flow regime depends on many factors including gas distributor type, gas density, liquid viscosity, and surface tension. Krishna et al. [26] pointed out that understanding the definition of the approximate transition point of the flow regime helps to understand and establish the hydrodynamic behavior in the bubble column.

To accurately design the bubble column and predict the flow regime in the column, it is often necessary to pay attention to the information related to the flow pattern transition parameters. Reilly et al. [27] proposed a correlation that can be used to estimate the gas holdup corresponding to the flow regime transition:

$$\varepsilon_{trans} = 0.59B^{1.5}\sqrt{\rho_g^{0.96}\sigma^{0.12}/\rho_l} \quad (7)$$

where the parameter B = 3.9. Although the correlation has a certain applicability, it does not consider the influence of liquid viscosity on the flow regime in the column. Wilkinson et al. [28] proposed a new correlation to identify the gas holdup in the process of flow regime transition. The specific expression is shown in Equation (8):

Preprints (www.preprints.org) | NOT PEER-REVIEWED | Posted: 8 November 2020 doi:10.20944/preprints202011.0258.v1

$$\varepsilon_{trans} = 0.5\exp\left(-6.1\rho_g^{-0.61}\mu_l^{0.5}\sigma_l^{0.11}\right) \quad (8)$$

The correlation also considers the influence of liquid surface tension and liquid viscosity on the flow regime transition, but its value is still very low in this experiment. The flow regime is not only determined by the physical properties of the fluid but is also closely related to the superficial gas velocity and the type of distributor. Wallis [29] proposed a drift flux theory to judge the flow regime, and modified the drift flux model to Equation (9):

$$U_w = U_g(1-\varepsilon_g)^{n-1} \pm U_l\varepsilon_g \quad (9)$$

where U_w is defined as the drift flux velocity, and n is the Richardson–Zaki index. In the low viscosity system, n = 2.39, and the value of n – 1 is close to 1. In the batch operation, U_l is 0. Therefore, the simplified equation is:

$$U_w = U_g(1-\varepsilon_g) \quad (10)$$

The size and velocity of the bubbles in the column of the acetic acid solution with different mass fractions are changed due to the physical properties, and it can then cause the flow regime to change in the bubble column. Figure 9 is the drift flux profile at 55–100% different acetic acid concentrations, drawn according to the drift flux velocity with the change in gas holdup. With the continuous increase in the acetic acid concentration in the bubble column, the flow regime transition point gradually moves forward, which indicates that with the increase in acetic acid concentration in the bubble column, the instability in the bubble column increases, leading to the advance of the transition point of the flow regime.

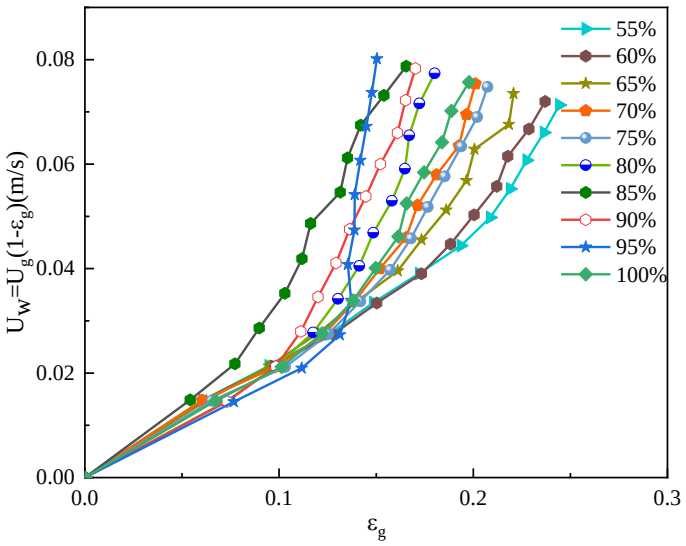

Figure 9 Flow characteristics analysis of the air-acetic acid system using drift flux analysis.

4. Conclusion

The experimental studies of air-acetic acid systems with different mass fractions are discussed in this article, and the following specific conclusions can be drawn.

（1）The physical properties of acetic acid solutions with different mass fractions are different,

 doi:10.20944/preprints202011.0258.v1

which changes the gas holdup in the column. The average gas holdup first increases and then decreases. When the mass fraction of acetic acid is between 55% and 60%, the gas holdup value is at its largest. The radial gas holdup distribution is more uniform. With an increase in the superficial gas velocity, the radial gas holdup appears to be high in the central regime and low in the wall. The radial gas holdup of different acetic acid concentrations has little difference at a low superficial gas velocity.

（2）The rising velocity of bubbles increases gradually with an increase in the superficial gas velocity, and the rising velocity of the bubbles in the column also shows the distribution pattern of a higher value in the central region and a lower value near the wall. The maximum rising velocity of bubbles is inversely proportional to the gas holdup in the column. Therefore, the higher the rising velocity of bubbles, the lower the gas holdup.

（3）In an air-acetic acid system with different mass fractions, the chord length distribution of the bubbles is relatively concentrated. In different radial positions, most bubbles are of a small size, which also shows that a decrease in the surface tension makes the chord length distribution of the bubbles in the column narrow.

Investigation: W.Z., S.N., L.M.; resources, S.N., X.G., R.Z.; data curation, S.N., W.Z., G.H.; writing—original draft preparation, W.Z.,S.N., G.H., L.M.,X.G., R.Z., H.J.; writing—review and editing, W.Z., S.N., H.J.; supervision, H.J.; project administration, H.J.

Funding: This research was funded by the National Natural Science Foundation of China, grant number 91634101, and The Project of Construction of Innovative Teams and Teacher Career Development for Universities and Colleges under Beijing Municipality, grant number IDHT20180508.

Conflicts of Interest: The authors declare no conflict of interest.

Nomenclature

λ_1	[mS cm^{-1}]	Conductivity of the continuous phase (acetic acid), mS cm^{-1}
λ_2	[mS cm^{-1}]	Conductivity of the dispersed phase (air), mS cm^{-1}
λ_{mc}	[mS cm^{-1}]	Conductivity value measured during the experiment, mS cm^{-1}
ε_g	[–]	Gas holdup
ε	[–]	Average gas holdup
ρ	[kg·m^{-3}]	Density, kg·m^{-3}
μ	[mPa·s]	Viscosity, mPa·s
σ	[N·m^{-1}]	Surface tension, N·m^{-1}
D	[mm]	The inner diameter of the bubble column, mm
g	[m·s^{-2}]	Gravitational acceleration, m·s^{-2}
H	[mm]	The height of the bubble column, mm
ΔH	[m]	Vertical distance between the two measurement sections, m
ΔP	[Pa]	Pressure difference measured between the two sections, Pa
L	[m]	Distance between the two probes, m
t_0	[s]	Time for the bubble to pass through the probe, s
r/R	[–]	Radial location
U_g	[m·s^{-1}]	Superficial gas velocity of air, m·s^{-1}
u_b	[m·s^{-1}]	Bubble rising velocity, m·s^{-1}

Lower Subscript

g	gas phase
l	liquid phase
i	referring to the gas phase or the liquid phase

References

[1] Krishna, R.; Urseanu, M. I.; Baten, J. M. V.; Ellenberger, J. Rise velocity of a swarm of large gas bubbles in liquids. *Chem. Eng. Sci.* **1999**, 54, 171-183. [CrossRef]

[2] Kulkarni, A. A.; Joshi, J. B. Bubble formation and bubble rise velocity in gas-liquid systems: a review. *Ind. Eng. Chem. Res.* **2005**, 44, 5873-5931. [CrossRef]

[3] Ning, S.; Jin, H.; He, G.; Ma, L.; Guo, X.; Zhang, R. Effects of the microbubble generation mode on hydrodynamic parameters in gas-liquid bubble columns. *Processes* **2020**, 8, 663. [CrossRef]

[4] Mandal, A.; Kundu, G.; Mukherjee, D. Gas holdup and entrainment characteristics in a modified downflow bubble column with Newtonian and non-Newtonian liquid. Chem. Eng. *Process* **2003**, 42, 777-787. [CrossRef]

[5] Mandal, A.; Kundu, G.; Mukherjee, D. A Comparative Study of Gas Holdup, Bubble Size Distribution and Interfacial Area in a Downflow Bubble Column. Chem. *Eng. Res. Des.* **2005**, 83, 423-428. [CrossRef]

[6] Guo, K.; Wang, T.; Yang, G.; Wang, J. Distinctly different bubble behaviors in a bubble column with pure liquids and alcohol solutions. *J. Chem. Technol. Biot.* **2016**, 92, 432-441. [CrossRef]

[7] Mouza, A. A.; Dalakoglou, G. K.; Paras, S. V. Effect of liquid properties on the performance of bubble column reactors with fine pore spargers. *Chem. Eng. Sci.* **2005**, 60, 1465-1475. [CrossRef]

[8] Kajero, O. T.; Azzopardi, B. J.; Abdulkareem, L. Experimental investigation of the effect of liquid viscosity on slug flow in small diameter bubble column. *EPJ Web of Conferences* **2012**, 25, 01037. [CrossRef]

[9] Prince, M J.; Blanch, H W. Bubble coalescence and break-up in air sparged bubble columns. *AIChE J.* **2010**, 36, 1485-1499. [CrossRef]

[10] Xing, C.; Wang, T.; Wang, J. Experimental study and numerical simulation with a coupled CFD-PBM model of the effect of liquid viscosity in a bubble column. *Chem. Eng. Sci.* **2013**, 95, 313-322. [CrossRef]

[11] Besagni, G.; Inzoli, F.; Guido, G. D.; Pellegrini, L. A. The dual effect of viscosity on bubble column hydrodynamics. *Chem. Eng. Sci.* **2017**, 158, 509-538. [CrossRef]

[12] Ruzicka, M. C.; Drahoš, J.; Mena, P. C.; Teixeira, J. A. Effect of viscosity on homogeneous -heterogeneous flow regime transition in bubble columns. *Chem. Eng. J.* **2003**, 96, 15-22. [CrossRef]

[13] Olivieri, G.; Russo, M. E.; Simeone, M.; Marzocchella, A.; Salatino, P. Effects of viscosity and relaxation time on the hydrodynamics of gas-liquid systems. *Chem. Eng. Sci.* **2011**, 66, 3392-3399. [CrossRef]

[14] Guan, X.; Yang, N. Bubble properties measurement in bubble columns: from homogeneous to heterogeneous regime. *Chem. Eng. Res. Des.* **2017**, 127, 103-127. [CrossRef]

[15] Parisien, V.; Farrell, A.; Pjontek, D.; McKnight, C. A.; Wiens, J.; Macchi, A. Bubble swarm characteristics in a bubble column under high gas holdup conditions. *Chem. Eng. Sci.* **2017**, 157, 88-98. [CrossRef]

[16] Zhang, T.; He, G.; Zhu, B.; Liu, L.; Han, Y.; Liu, M.; Jin, H. Measurement of solid holdup in gas-solid flow using optical fiber probe. *Acta. Pet. Sin.* **2019**, 35, 66-72. [CrossRef]

[17] Suard, E.; Clément, R.; Fayolle, Y.; Alliet, M.; Albasi, C.; Gillot, S. Electrical resistivity tomography used to characterize bubble distribution in complex aerated reactors: Development of the method and application to a semi-industrial MBR in operation. *Chem. Eng. J.* **2019**, 355, 498-509. [CrossRef]

[18] Stanley, S. J.; Bolton, G. T.; A Review of recent electrical resistance tomography (ERT) applications for wet particulate processing. *Part. Part. Syst. Char.* **2008**, 25, 207-215. [CrossRef]

[19] Jin, H.; Wang, M.; Williams, R. Analysis of bubble behaviors in bubble columns using electrical resistance tomography. *Chem. Eng. J.* **2007**, 130, 179-185. [CrossRef]

[20] Jin, H.; Han, Y.; Yang, S. Gas-Liquid flow characterization in bubble columns with various gas-liquid using electrical resistance tomography. *J. Phys. Conf. Ser.* **2009**, 147, 012032. [CrossRef]

[21] Zhang, T.; He, G.; Zhu, B.; Liu, L.; Han, Y.; Liu, M.; Jin, H. Measurement of solid holdup in gas-solid flow using optical fiber probe. *Acta Petrolei Sinica: Petroleum Processing Section* **2019**, 35, 268-274. [CrossRef]

[22] Kim, J.; Kim, B.; Nho, N.; Go, K.; Kim, W.; Bae, J.; Jeong, S.; Epstein, N.; Lee, D. Gas holdup and hydrodynamic flow regime transition in bubble columns. *J. Ind. Eng. Chem.* **2017**, 56, 450-462. [CrossRef]

[23] Patel, S. A.; Daly, J. G.; D. Bukur, B. Bubble-size distribution in Fischer-Tropsch-Derived waxes in a bubble column. *AIChE J.* **1990**, 36, 93-105. [CrossRef]

[24] Grevskott, S.; Sannæs, B. H.; Dudukovi, M. P.; Hjarbo, K. W.; Svendsen, H. F. Liquid circulation, bubble size distributions, and solids movement in two- and three-phase bubble columns. *Chem. Eng. Sci*. **1996**, 51, 1703-1713. [CrossRef]

[25] Polli, M.; Stanislao, M. D.; Bagatin, R.; Bakr, E. A.; Masi, M. Bubble size distribution in the sparger region of bubble columns. *Chem. Eng. Sci.* **2002**, 57, 197-205. [CrossRef]

[26] Krishna, R.; Wilkinson, P. M.; Dierendonck, L. L. V. A model for gas holdup in bubble columns incorporating the influence of gas density on flow regime transitions. *Chem. Eng. Sci.* **1991**, 46, 2496-2509. [CrossRef]

[27] Reilly, I. G.; Scott, D. S.; de Bruijn, T. J. W.; MacIntyre, D. The role of gas phase momentum in determining gas holdup and hydrodynamic flow regimes in bubble column operations. *Can. J. Chem. Eng.* **1994**, 72, 3-12. [CrossRef]

[28] Wilkinson, P. M.; Spek, A. P.; Dierendonck, L. L. Design parameters estimation for scale-up of high-pressure bubble columns. *AICHE J.* **1992**, 38, 544-554. [CrossRef]

[29] Wallis, G. B. One-dimensional two-phase flow. McGraw-Hill. **1969**.